Novel Concepts for Slow Wave Structures used in High Power Backward Wave Oscillators

By

Ushemadzoro Chipengo

Abstract

This proposal presents novel slow wave structure (SWS) designs and concepts that have been developed to significantly improve the efficiency and performance of high power backward wave oscillators (BWOs). A novel slow wave structure design is presented. The design features a deeply corrugated cylindrical waveguide with cavity recessions and metallic ring insertions. A new technique for mode control in waveguides is also presented. In addition to demonstrating mode control in slow wave structures, the key aspects of the presented design are mode dominance reversal and a 100% improvement in interaction impedance. A novel and cost efficient fabrication technique for the SWS is presented. Fabrication and testing results are also presented to experimentally validate the dispersion properties of the novel SWS. Furthermore, we experimentally demonstrate, for the first time, mode dominance reversal in SWSs. We extend the concepts of inhomogeneous SWSs by designing a 3-section inhomogeneous SWS to further enhance the BWO energy conversion efficiency. Results from commercial particle in cell codes predict an output power of 5.92 MW at 27 GHz with 58% peak power efficiency. Further S band simulations using the concepts outlined above predict 8.25 MW output power at 2.62 GHz with 70% peak power efficiency. These results must be compared to the 20-25% peak power efficiency associated with conventional slow wave structure designs. Future work will be focused on designing and fabricating a full SWS and coupler for a hot test experiment at the M.I.T Plasma Science and Fusion Center. Multi-section (more than 3 sections) inhomogeneous SWS behavior will be investigated and characterized in regards to BWO efficiency enhancement. New methods of efficiently operating BWOs under low magnetic field conditions will also be investigated. High frequency SWS design solutions for high efficiency operation will be investigated.

Table of Contents

1. Introduction

Backward wave oscillators (BWOs) are O-type, Cerenkov radiation based, high power microwave sources that convert the energy of a high power electron beam into RF power. These devices find application in plasma science, electronic warfare (Active Denial System- ADS), high power radar (Nanosecond Gigawatt Radar- NaGiRa system) and electronic system susceptance and vulnerability testing. Devices have been developed in S band to terahertz frequencies [1]- [7], producing mW to GW of RF power. The interest in these devices has been mainly because BWOs offer high power, a robust design and high repetition rates at modest efficiencies of 20-25% when using conventional slow wave structures (SWSs).

BWO operation is based on coherent Cerenkov radiation. Cerenkov radiation is the phenomenon that arises when an electron travels in a medium at a velocity slightly greater than the local phase velocity of electromagnetic waves in that medium. This means that the velocity of electrons in the electron beam must be matched to the phase velocity of an electromagnetic wave to achieve Cerenkov radiation. For high power, waveguides are the obvious transmission lines of choice, therefore, waveguides provide the default interaction medium for high power Cerenkov radiation. However, as is well known, the phase velocity of electromagnetic waves in waveguides is greater than *c*. This condition makes velocity synchronism of electrons in the beam with the electromagnetic wave impossible since the electrons cannot be physically accelerated to velocities greater than *c*. Slow waves structures alleviate the above stated synchronism issue by significantly reducing the phase velocity of the electromagnetic wave to velocities that can be reached by the electrons for synchronism. Therefore, SWSs are an essential component of the BWO system since they guide the electromagnetic mode while concurrently matching wave velocity to the electron beam velocity. Various types of SWSs have been designed for BWOs. By varying the corrugation

profiles of cylindrical waveguides, sinusoidal, rectangular, trapezoidal and semicircular profiles have been employed in BWO SWSs [8]-[11].

Although BWOs can generate MW to GW of power, they still suffer from poor energy conversion efficiency and low output mode purity. Specifically, the nominal electronic efficiency of BWOs employing homogeneous SWSs is 20-25% [12]-[15]. Therefore, there is a need to enhance the efficiency of BWOs while improving the output mode purity. An immediate advantage of improving the energy conversion efficiency will be the miniaturization of the overall BWO system. Specifically, improving efficiency reduces the input beam power required to produce a constant amount of output power. A reduction in the input beam power leads to lower beam voltages, beam currents and consequently smaller beam confining magnets.

Many efforts have been made to improve the efficiency of BWOs. However, most of these techniques employ the conventional, corrugated cylindrical waveguide or slight modifications with sometimes imperceptible changes to the fundamental dispersion properties of the SWS. This has led to slight improvements in the efficiency of BWOs. In light of this, our research efforts have been focused on introducing a novel SWS design with game changing electromagnetic properties that can significantly improve the efficiency of BWOs while simultaneously yielding an output mode with high spectral purity.

In this proposal, we present a recently developed, novel SWS design that features a deeply corrugated, cylindrical waveguide with cavity recessions and metallic ring insertions. This design provides higher interaction impedance, increased flexibility in dispersion curve engineering and improved mode control capabilities. As we will demonstrate, these properties can be exploited to enhance the efficiency of BWOs and improve the output mode purity. Furthermore, we will present a cheap fabrication technique that accurately reproduces the otherwise complex axial profile of the

new SWS design. Using this fabricated SWS, the dispersion properties of the novel SWS were validated with high accuracy. In addition, mode dominance reversal, a key novelty of our SWS was experimentally validated. Recently developed efficiency enhancement concepts of 3-section inhomogeneous SWSs will be presented and shown to realize efficiencies of over 70% in PIC code simulations. Finally, we will present the fabrication and cold testing of a 3-section inhomogeneous SWS. Results from this cold test demonstrated, for the first time, multiple secondary inflexion points (MSIPs) dispersion.

Future work will be focused on hot tests. That is, we will seek to introduce a high power electron beam into the SWS and validate the output power previously predicted by PIC codes. These hot tests will be carried out at the M.I.T. Plasma Science and Fusion Center. Inhomogeneous SWSs have shown great promise in enhancing BWO efficiency, therefore, future work will focus on methodically determining the most efficient inhomogeneous SWS configuration using multiple SWS sections. Low magnetic fields are known to reduce the efficiency of BWOs. Therefore, novel techniques for efficiently operating BWOs under low magnetic fields will also be investigated. As BWOs move to higher frequencies, a physical reduction in the SWS size leads to very low efficiencies (<10%). In light of this, future work will also focus on design techniques that can significantly improve the efficiency of BWOs at W band frequencies and beyond.

2. Competing Technologies and State of the Art MVEDs

BWOs belong to a family of devices known as microwave vacuum electron devices (MVEDs). The peak and average output powers of MVEDs are much greater than those of the competing solid state device (SSDs) technology. Fig.1 shows the state of the art output powers of both MVEDs and SSDs versus the operating frequency [16]. SSDs are cheaper to fabricate and also allow mass

manufacturing due to the inherent nature of solid state technology. SSDs are also compact and much lighter than VEDs [17]. On the other hand, SSDs offer significantly less power than MVEDs with severely degrading performance as frequency increases. In addition, MVEDs can reliably operate at much higher temperatures than SSDs with a much higher efficiency [18]. Therefore, for applications such as satellite communications where high power, reliable operation with extremely high mean time between failures (MTBF) under harsh conditions is required, MVEDs are the devices of choice. As an example, a comparison of two fairly similar radar systems employing SSDs (SPS-40E) and MVEDs (AN/SPY-1) was made. When transitioning from the MVED radar system to the SSD radar system, a 50% reduction in radar range and system availability was observed. Furthermore, the support costs *increased* by a factor of 5 [17].

Among other MVEDs are some competing devices such as klystrons, travelling wave tube amplifiers (TWTA), gyrotrons and crossed field amplifiers. Klystrons are capable of producing high power comparable to BWOs, however they have a very small tunable bandwidth (<1%). TWTAs have wide bandwidth, however, the break into oscillations at high powers thus limiting their output power. Gyrotrons produce higher output power than BWOs, however their dependence on strong magnetic fields makes them extremely bulky. Crossed field amplifiers have wider bandwidth but less output power when compared to BWOs. Table 1 shows state of the art MVEDs.

TABLE 1
State of the Art MVEDs

Device	Manufacturer	Performance
Klystron [19]	L3 Electron Devices	2.856 GHz, 5.5 MW, 47% Efficiency (With Depressed Collector), 0.03% Bandwidth
Magnetron [20]	L3 Electron Devices	2.805 GHz, 4.5 MW, 49% Efficiency (With Depressed Collector)
Travelling Wave Tube Coupled Cavity [21]	L3 Electron Devices	3.1-3.5 GHz, 125 kW, 35% Efficiency
Klystron [22]	Communications and Power Industries (CPI)	2.856 GHz, 5.5 MW, 49% Efficiency (With Depressed Collector)
Travelling Wave Tube[23]	Communications and Power Industries (CPI)	3.1-3.5 GHz, 160 kW, 20% Efficiency
Gyrotron [24]	Communications and Power Industries (CPI)	28 GHz, 200 kW, 31 % Efficiency
Resonant Backward Wave Oscillator [1]	National University of Defense Technology, China	3.62 GHz, 1GW, 20% Efficiency
Backward Wave Oscillator (Proposed Design)	**The Ohio State University**	**2.62 GHz, 8.25 MW, 70% Efficiency (3-section inhomogeneous SWS-no depressed collector)**

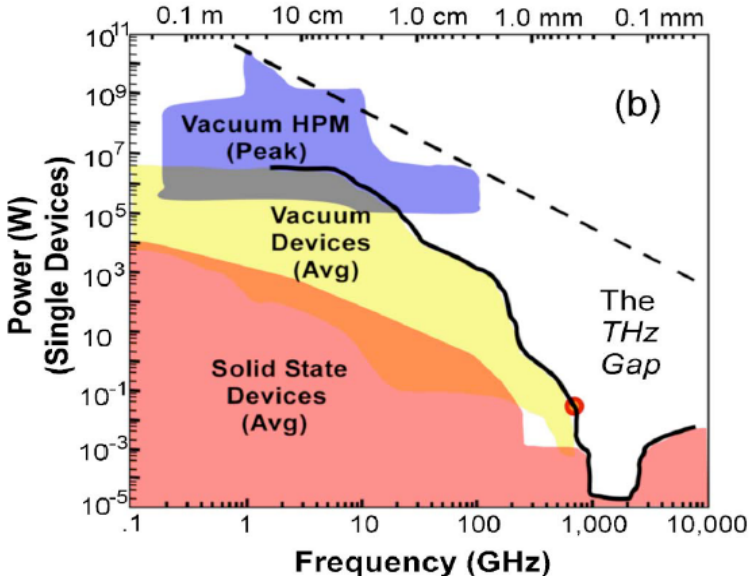

Figure 1. Power vs Frequency for solid state devices and vacuum electron devices [16]

3. Literature Review

As highlighted earlier, BWOs function by converting the energy of a high power electron beam into RF power. A key area of research has been the improvement of the basic electronic efficiency of BWOs. Specifically, we seek to increase the amount of beam power that is converted to RF power. The immediate advantage of efficiency enhancement would be overall device miniaturization. This is because, smaller currents and smaller beam voltages translate to smaller prime power sources. In addition, a reduction in beam current translates to a reduction in the guiding magnetic field strength. With smaller magnets, the overall BWO system can be further miniaturized while reducing the BWO power consumption since the solenoids are extremely heavy, bulky and consume a lot of power.

With these advantages in mind, efficiency enhancement efforts have been in two directions. The first direction is that of depressed collectors. The collector is the structure inside the BWO where the electron beam is deposited after interacting with the electromagnetic wave inside the SWS. A depressed collector consists of reverse biased electrodes that slow down the electron beam before its is deposited. The recovered kinetic energy is fed back to the power supply thus effectively reducing the wasted beam energy at the collector [18]. Depressed collectors have been used to improve the overall device efficiency to over 50% however, they cannot improve the more critical electronic conversion efficiency. Furthermore, they are usually employed as multistage collectors which are complex and expensive.

The second area of research has been focused on developing SWS designs that enhance the electron beam and electromagnetic wave interaction. SWS design directly impacts the electronic conversion efficiency since beam-mode energy exchange occurs within the SWS. Various efficiency enhancing techniques have been investigated to date. Plasma filled BWOs have been

developed in a bid to enhance the interaction impedance with efficiencies of 30% being realized [25]-[27]. An efficiency of 40% has been attained in a plasma injected BWO [28]. End reflections in BWO SWSs have been used to enhance the efficiency. In this scheme, shorting plates have been placed at the electron gun end of the BWO to vary and optimize the phase of the reflected wave at the collector end of the SWS. This reflected wave can then constructively or destructively interfere with the backward wave inside the SWS yielding efficiencies of 30-40% [29]-[31]. Metamaterials have been employed in BWOs, however, these metamaterial-based BWOs promised efficiencies of around 14% [32]. Cutoff waveguides and resonant reflectors have been used to allow efficient operation of BWOs under extremely high power operation. Specifically, 5 GW was produced at S-band with 30% efficiency [5].

Inhomogeneous SWSs have shown great promise as a means of significantly enhancing the efficiency of BWOs [14]-[15]. By varying the interaction impedance and phase velocity profiles along the SWS length, an optimum profile for beam-mode interaction leads to significant efficiency enhancement. Numerical calculations have predicted efficiencies of 70% while 45% has been realized experimentally [33] with 2-section SWS. These discrepancies can be because these numerical calculations were not full PIC simulations that incorporate space charge. Recently, we introduced a 3-section inhomogeneous SWS that demonstrated 58% efficiency at 27 GHz [34] using CST PIC code simulations. We also note that an S-band scaled version of this SWS demonstrated 70% efficiency. These results demonstrate that inhomogeneous SWSs are the most promising and cost effective method of significantly increasing the basic electronic efficiency of BWOs.

4. Research Accomplishments

4.1 Slow Wave Structures Theory

The energy exchange between the electron beam and the operational TM_{01} mode occurs inside a SWS. Fig. 2 shows the SWS region of the BWO system. The SWS is a periodic structure whose operation can be described by using Floquet's theorem. This theorem states that the steady state solutions for electromagnetic fields within adjacent cells of a periodic structure vary only by a complex constant. This constant is the same for all the pairs of adjacent cells [35]. This can be expressed as

$$\boldsymbol{E}(x, y, z - d) = e^{jk_0 d}\boldsymbol{E}(x, y, z) \qquad (1)$$

where k_0 is the propagation constant which can be complex and d is periodic length. If the periodic structure is lossless, then k_0 is real. The electric field is therefore periodic in the z direction and can be expressed as:

$$\boldsymbol{E}(x, y, z) = \boldsymbol{E_p}(x, y, z)\, e^{-jk_0 z} \qquad (2)$$

Therefore, because E_p is periodic in z, it can be presented by a Fourier series

$$\boldsymbol{E_p}(x, y, z) = \sum_{n=-\infty}^{\infty} \boldsymbol{E_n}(x, y, z) e^{-jk_n z} \qquad (3)$$

where n is the spatial harmonic number. Therefore, a single mode consists of an infinite number of space harmonics. Each space harmonic satisfies Maxwell equations, however only the full set of space harmonics satisfies the boundary conditions imposed by the SWS walls.

$$k_n = k_0 + \frac{2\pi n}{d} \qquad (4)$$

The phase velocity $v_{phase,n}$ of the n^{th} space harmonic is

$$v_{phase,n} = \frac{\omega}{k_n} \qquad (5)$$

where ω is the angular frequency of the propagating mode. When $k_n > k_0$, the resulting phase velocity of the wave is less than c. Therefore, the propagating mode is called a slow wave.

Backward wave oscillators convert the energy of a high power electron beam into RF power via the Cerenkov radiation mechanism. For Cerenkov radiation to take place, the velocity of electrons in the beam must match the phase velocity of one of the space harmonics of the interacting TM_{01} mode. This can be expressed as:

$$\omega - k_{z,1}^{-} v_z \approx 0 \qquad (6)$$

where v_z is the velocity of electrons in the beam and $k_{z,1}^{-}$ is the longitudinal wavenumber of the *n=1* spatial harmonic of the backward wave. By using (5) and (6), the Cerenkov synchronism condition can simply be expressed as:

$$v_{phase(wave)} \approx v_{z(beam)} \qquad (7)$$

Having established the phase velocity of the SWS, the remaining key parameter is the interaction impedance. The beam-mode interaction in the BWO requires a mode with strong E_z electric field

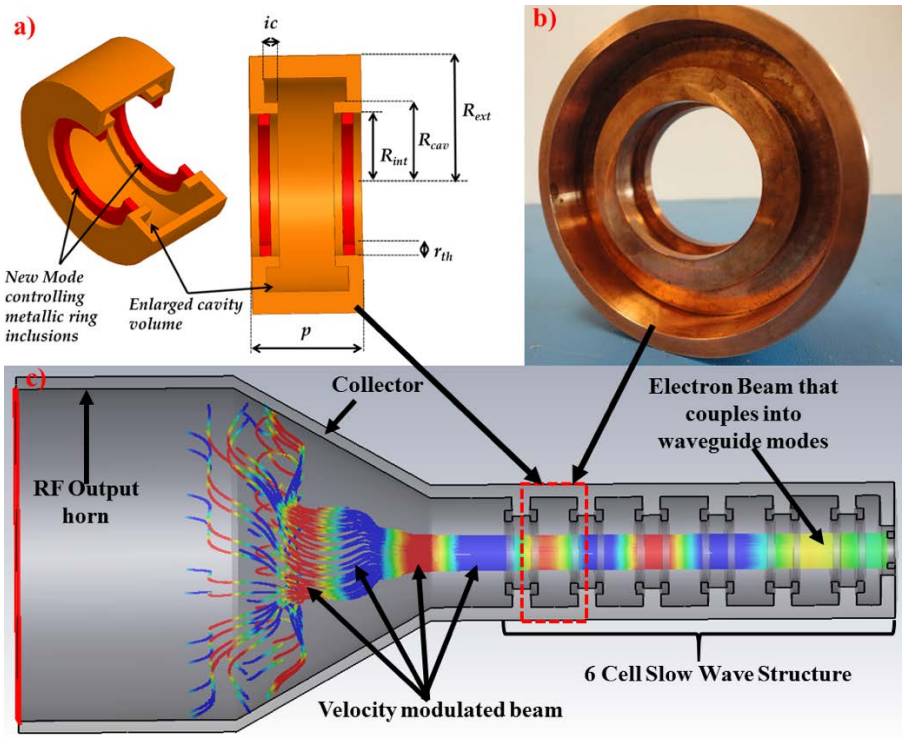

Fig. 2: Full backward wave oscillator system and working principles. a) Novel SWS design, b) Fabricated single cell of SWS c) Full SWS featuring 6 cells of the proposed SWS cell design.

components. Therefore, for the beam and mode to couple, a TM_{01} mode is used due to its strong E_z component. The interaction impedance K_{cn} (Ω) is a parameter that describes the intensity of the beam-mode interaction [36]. High interaction impedance leads to high electronic efficiency, therefore, the SWS design must have high interaction impedance in the frequency band of operation. Interaction impedance is given by:

$$K_{cn} = \frac{|E_{zn}|^2}{2k_{zn}^2 P} \qquad (8)$$

where E_{zn} is the z-component of the n^{th} space harmonic. P is the total TM_{01} mode power flowing inside the SWS. To calculate E_{zn}, a spatial Fourier decomposition of the total field must be taken, we begin by noting that:

$$E_z = \sum_{n=-\infty}^{n=\infty} E_{zn}(x,y)e^{-jk_{zn}z} \qquad (9)$$

Therefore

$$|E_{zn}| = \frac{1}{d}\left|\int_0^d (E_{zr}(z) + jE_{zi}(z))e^{jk_{zn}z}\right| \quad (10)$$

This can be implemented in HFSS by invoking Euler's identity:

$$e^{jk_{zn}z} = \cos(k_{zn}z) + jsin(k_{zn}z) \quad (11)$$

Finally this yields,

$$|E_{zn}| = \frac{1}{d}\left|\int_0^d \left(E_{zr}(z) + jE_{zi}(z)\right) * (\cos(k_{zn}z) + jsin(k_{zn}z))\right| \quad (12)$$

4.2 BWO Working Principles

In BWO operation, a high power electron beam with voltage V_0 and current I_0 is injected into a SWS by a space charge limited electron gun. This electron beam is guided by a strong magnetic field as it traverses the SWS length. After the energy exchange has occurred inside the SWS, the spent beam is deposited on the walls of the output horn that serve as the collector. Due to the backward nature of the wave in the BWO, the TM_{01} mode grows in the direction of the electron gun. The growing backward wave is reflected at the gun end of the SWS where it becomes a forward wave that exits the SWS through the RF output horn. This interaction process is explained by 3 representative equations, namely the electronic, circuit and determinantal equations.

4.2.1 The Electronic Equation

The electronic equation provides a relationship between the induced RF current on the electron beam and the voltage on the SWS as represented by the electric field of the synchronous space harmonic [35]. Specifically, the electronic equation shows how the electric field E_{zn} on the SWS induces currents i on the electron beam. [18]

$$i = \frac{j\beta_e I_0 E_{zn}}{2V_0\left[(\Gamma - j\beta_e)^2 + \frac{\omega_q^2}{u_0^2}\right]} \qquad (13)$$

where ω_q is the reduced plasma frequency ω_p which is given by:

$$\omega_p = \sqrt{\frac{n_e e^2}{m\varepsilon_0}} \qquad (14)$$

where n_e, e, m and ε_0 is the electron number density, electron charge, electron mass and permittivity of free space. β_e is the electron phase constant given by ω/v_z. Finally, Γ is the complex valued propagation constant of the possible waves that can propagate in the SWS.

4.2.2 The Circuit Equation

The circuit equation provides a relationship between the RF currents on the electron beam and the voltages that they induce on the SWS as represented by the electric field of the synchronous space harmonic [35]. Specifically, the circuit equation shows how the RF currents on the electron beam represented by *i* can lead to electric fields E_z on the SWS [18].

$$(\Gamma^2 - \Gamma_0^2)E_{zn} = -\Gamma_0 k_{zn}^2 K_{cn} i \qquad (15)$$

where $\Gamma_0 = \alpha + jk_{zn}$ is the complex propagation constant of the SWS in the absence of the electron beam while Γ is the complex valued propagation constant of the possible waves that can propagate in the SWS. K_{cn} is the interaction impedance as given by (8).

4.2.3 The Determinantal Equation

$$(\Gamma^2 - \Gamma_0^2)\left[(\Gamma - j\beta_e)^2 + \frac{\omega_q^2}{u_0^2}\right] = \frac{-j\beta_e\beta_n^2\Gamma_0 K_{cn} I_0}{2V_0} \qquad (16)$$

The D.C. electron beam excites an electromagnetic wave (TM_{01} for BWOs) within the SWS. This excited mode grows and its electric field interacts with the electron in the beam. Depending on the particular phase of the electric field at a specific point, some electrons are accelerated and some are decelerated. This velocity modulation leads to bunching of the electron beam (see Fig.2). This modulated electron beam now represents a modulated RF current that further induces currents on the SWS. This symbiotic relationship continues until saturation. Solving the determinantal equation therefore provides the values of the "hot" propagation constants that can sustain this cumulative interaction.

4.3 Design of a Novel SWS with Mode Control

4.3.1 SWS Design

As previously stated, SWS design improvement has proven to be the most promising and cost efficient method of significantly enhancing the basic electronic conversion efficiency of BWOs. Recently, we showed that the basic efficiency of BWOs can be improved by increasing the interaction impedance of the SWS [34]. The conventional SWS is a simple corrugated cylindrical waveguide as shown in Fig.3. Interaction impedance of conventional, corrugated SWSs can be increased by deepening the corrugations. However, overlapping passbands still exist between the TE_{11} and TM_{01} modes. Overlapping passbands reduce the interaction impedance since they lead to low mode purity. Specifically, reflections at the SWS corrugations edges can lead to the excitation of multiple modes at the same frequency. In BWO operation, the mode of interest is the TM_{01} mode, however, when mode passband overlap exists, the resulting hybrid mode is usually a superposition of TE_{11} and TM_{01} modes.

This resulting hybrid mode has weaker E_z fields which subsequently lead to lower interaction impedance as shown by equation (8). Low interaction impedance limits the conversion efficiency of BWOs. Furthermore, overlapping passbands limit the output mode purity. To address these challenges, we designed a SWS that features a deeply corrugated cylindrical waveguide with enlarged cavity recessions and metallic ring insertions. The key properties of this SWS are mode dominance reversal, clear mode isolation leading to excellent mode purity and high interaction impedance.

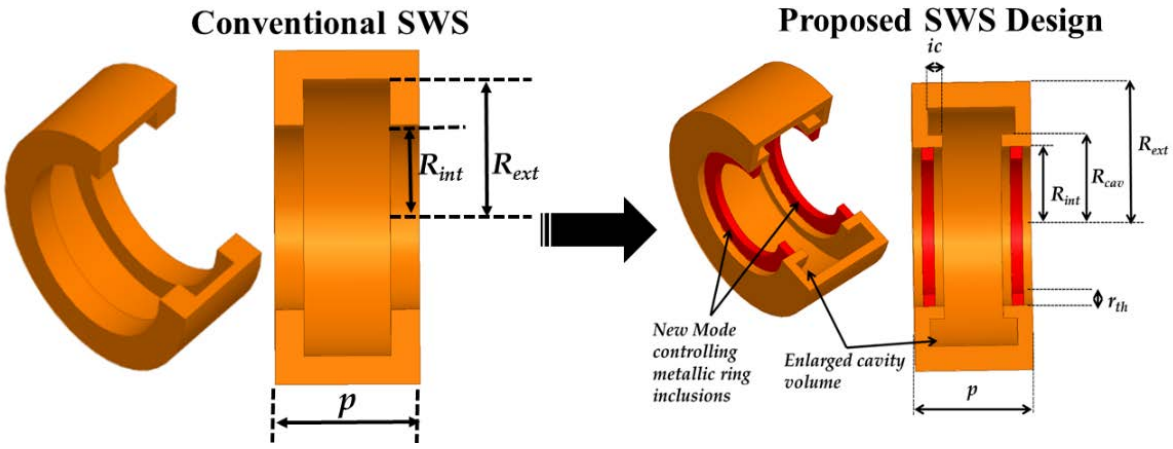

Fig.3: Conventional SWS design vs Proposed SWS with cavity recessions and metallic ring insertions.

4.3.2 Mode Dominance Reversal

Although the TM_{01} mode is the operational mode inside the SWS, it is not the dominant mode. Specifically, the TE_{11} mode is the first mode to be excited, then followed by the TM_{01} mode. To improve the mode purity and subsequent interaction impedance, we designed the novel SWS to favor excitation of the TM_{01} mode. Specifically, to ensure excellent mode purity, we designed a SWS that flipped the TE_{11} and TM_{01} modes' frequency order of appearance in the SWS thus making the TM_{01} mode dominant inside the SWS. We coined the term mode dominance reversal

to this breakthrough phenomenon (see Fig. 4). Furthermore, we eliminated the mode overlap between the passbands of the TE_{11} and TM_{01} modes.

Fig. 4 shows the full S Band dispersion curves of the conventional and proposed SWS along with the resulting electric fields when the SWSs are given an arbitrary excitation. As can be seen, the proposed SWS supports a pure TM_{01} mode due to mode dominance reversal and isolated mode passbands. On the other hand, the conventional SWS supports a hybrid mode with evidently weaker E_z fields and poor TM_{01} mode purity. Both mode dominance reversal and mode passband isolation were achieved by independently controlling the dispersion properties of the TE_{11} and TM_{01} modes due to their different field distributions. Specifically, the cavity recessions affected the TM_{01} mode while the metallic ring insertions primarily affected the TE_{11} mode.

4.3.3 Interaction Impedance Enhancements

The interaction impedance of SWSs quantitatively depicts the beam-mode interaction intensity and is defined using (8). Mode dominance reversal and mode passband isolation lead to an interaction impedance enhancement. Both these phenomena improve the strength of the E_z field component thus improving the interaction impedance. Fig.5 shows the interaction impedance enhancement. As can be seen, the interaction impedance of the proposed SWS is over twice that of conventional SWSs for most frequencies. This can be attributed to the stronger E_z fields that resulted from mode dominance reversal and passband overlap elimination as highlighted earlier (see Fig. 4).

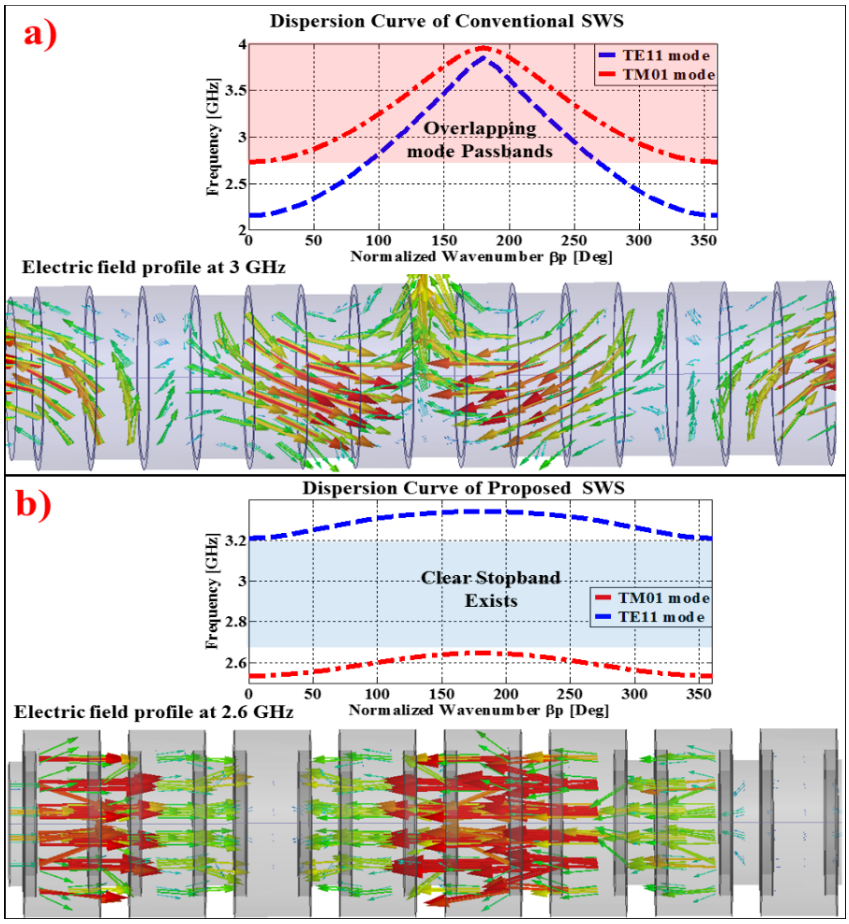

Fig. 4: Dispersion plots and field profiles for a) conventional SWS and b) proposed SWS with mode dominance reversal and mode isolation.

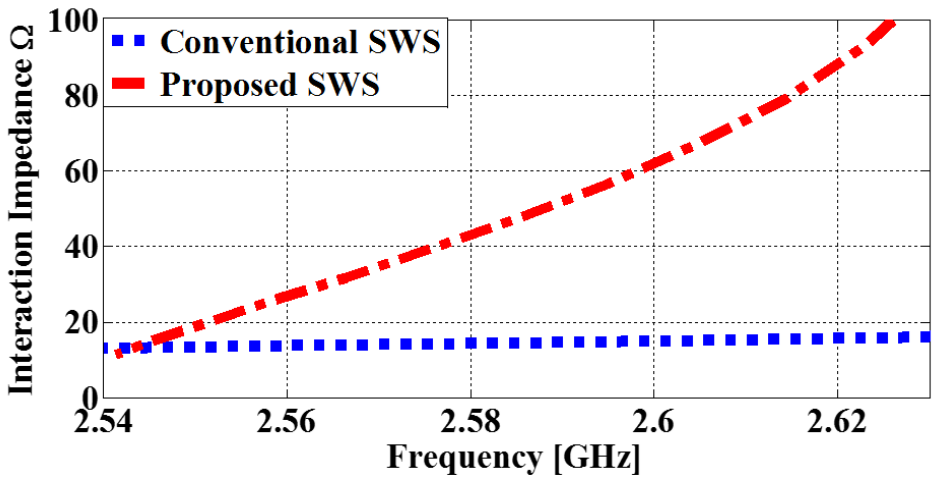

Fig. 5: Interaction impedance of Conventional vs Proposed SWS.

4.4 Fabrication and Cold Testing of SWS

4.4.1 Novel Fabrication Technique

Although the SWS design promised novel electromagnetic properties, the physical realization of this design remained as a challenge. Specifically, the cavity recessions and metallic ring inclusions are hard to realize with conventional fabrication techniques. Another technique that can be used is electroforming, however, it is an expensive and time consuming process. To address these issues, we came up with a novel fabrication technique to realize the SWS design as shown in Fig. 6 [37]. The fabrication technique consisted of 3-steps that include periodicity plane shift, metallic ring integration and waveguide loading. We viewed the SWS as a smooth waveguide loaded with single SWS unit cells to realize the full profile. Fabricated components are shown in Fig.7.

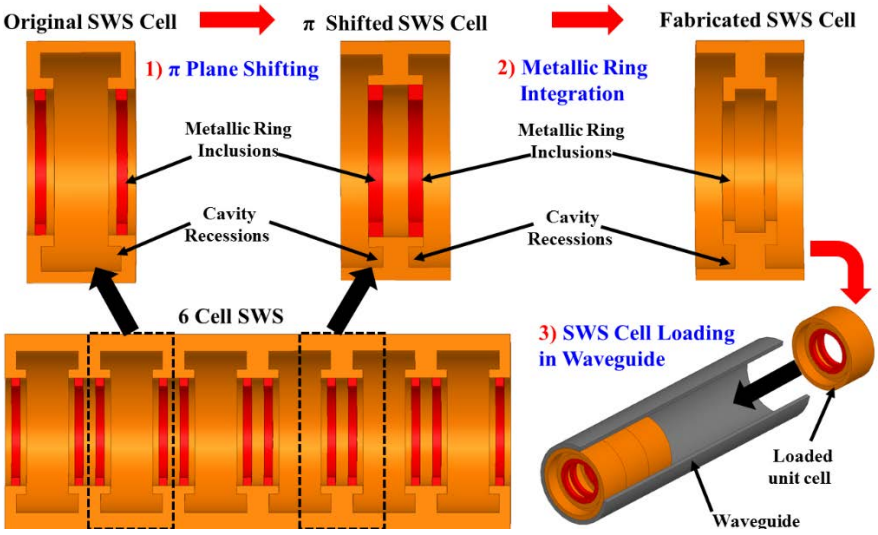

Fig.6: Proposed Fabrication Technique

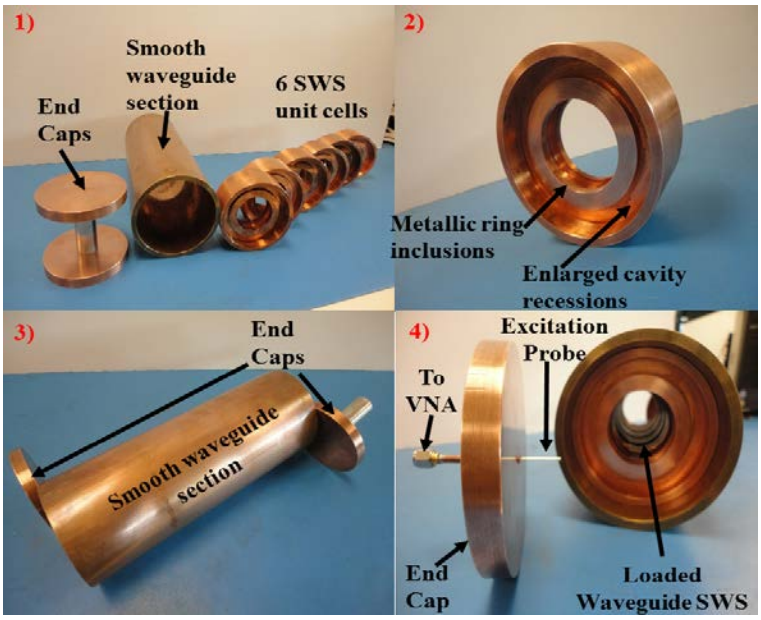

Fig.7: Fabricated SWS components for cold testing

4.4.2 Cold Test Validation of Dispersion Properties

As is well known, an *n* period SWS will exhibit *n+1* resonances when shorted at the ends and excited appropriately. These resonances can then be used to derive the weighting coefficients of a sum of sinusoids that describe the full dispersion relation. Using a highly accurate synthetic technique by Guo et al. [38], we cold tested our SWS to validate the dispersion properties. Fig. 8 shows the experimental setup where an excitation probe connected to a VNA is used to excite and measure the resonances. Fig. 9 shows the measurement results compared to the simulated results from commercial software CST and HFSS. As seen, there is excellent agreement between simulated and measured results.

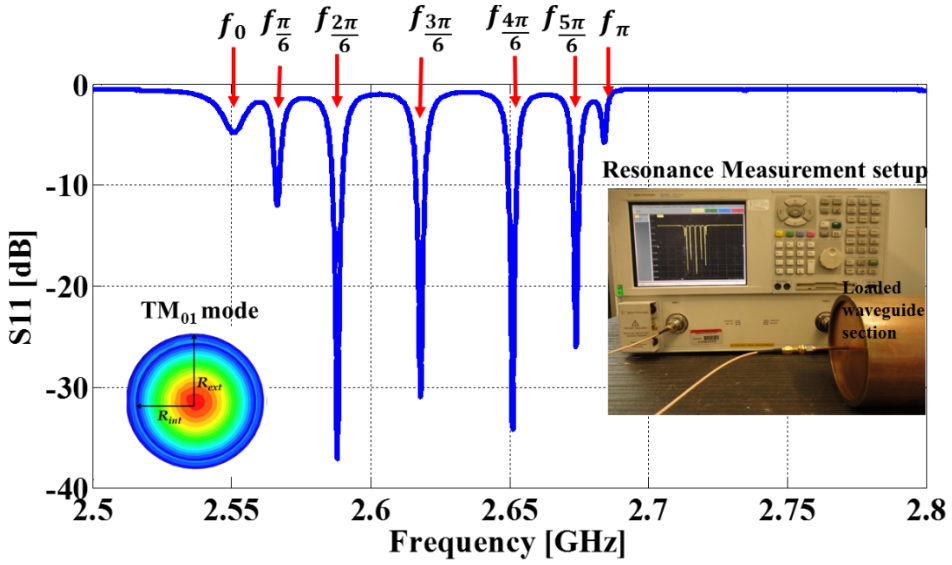

Fig 8: Measured resonance and experimental setup.

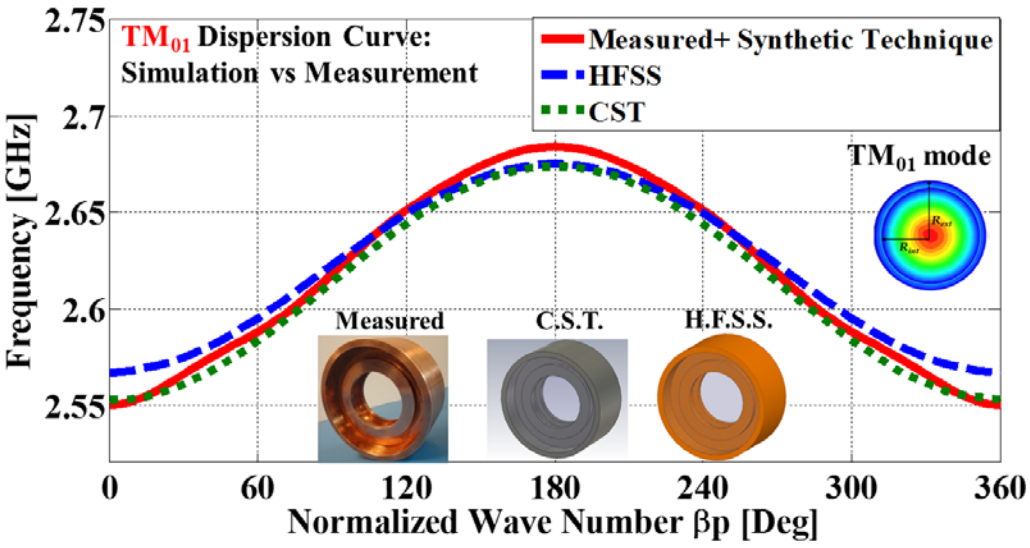

Fig. 9: Full Dispersion Curve of TM_{01} mode, measured vs simulated results.

4.4.3 Experimental Validation of Mode Dominance Reversal

As mentioned earlier, the new SWS has high interaction impedance and excellent mode purity. These properties can be attributed to mode dominance reversal and isolated mode passbands, both of which had never been validated experimentally. To validate these properties, we excited the SWS over a larger frequency range (1-4GHz), measured the S_{11} and then mapped the dispersion

curves to the S_{11} data. Fig. 10 shows the color coded full dispersion curves of the TM_{01} and TE_{11} modes while Fig. 11 shows the color coded S_{11} data. As can be seen, clear stopbands exist between the position of the already confirmed TM_{01} resonances and the weakly excited TE_{11} resonances thus validating the proposed electromagnetic qualities.

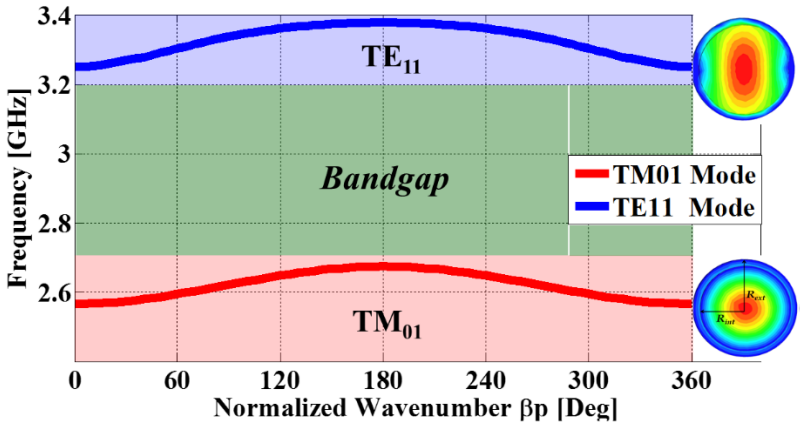

Fig. 10: Dispersion Curves of TM_{01} and TE_{11} modes.

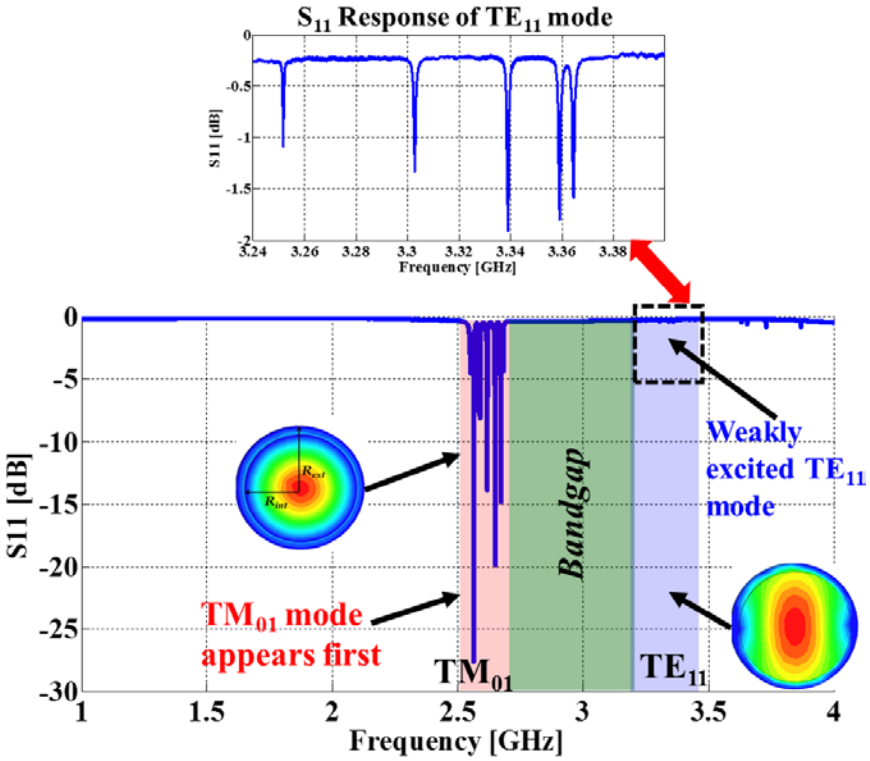

Fig.11: Measured S_{11} data for 6 cell SWS.

4.5 3-Section Inhomogeneous SWS and Multiple Secondary Inflexion Points MSIPs

Inhomogeneous SWS have long been used to enhance the electronic efficiency of BWOs. By varying the phase velocity and interaction impedance of the propagating mode, an optimum profile can be created to ensure that the beam loses more energy to the electromagnetic mode. 2-section SWSs have long been used [14]-[15] however, their efficiency is limited due to impedance mismatch at the SWS section junctions. To further improve the phase velocity and interaction increments while avoiding impedance mismatches, we introduced 3-section a inhomogeneous SWS. This SWS design enhances efficiency through its higher order dispersion properties. Specifically, 3-section SWS have MSIPs that are characterized as low group velocity points. Low group velocity points to low power flow and hence increases interaction impedance as shown by equation (8). Fig. 12 shows the fabricated 3 SWS cells while Fig. 13 shows the dispersion properties of inhomogeneous SWSs compared to homogeneous SWSs. We note that Fig. 13 is the first demonstration, to our knowledge of MSIPs in SWSs for BWOs.

Fig.12: 3 SWS cells with differing periods (p=45mm, 55mm and 65mm) for an inhomogeneous SWS.

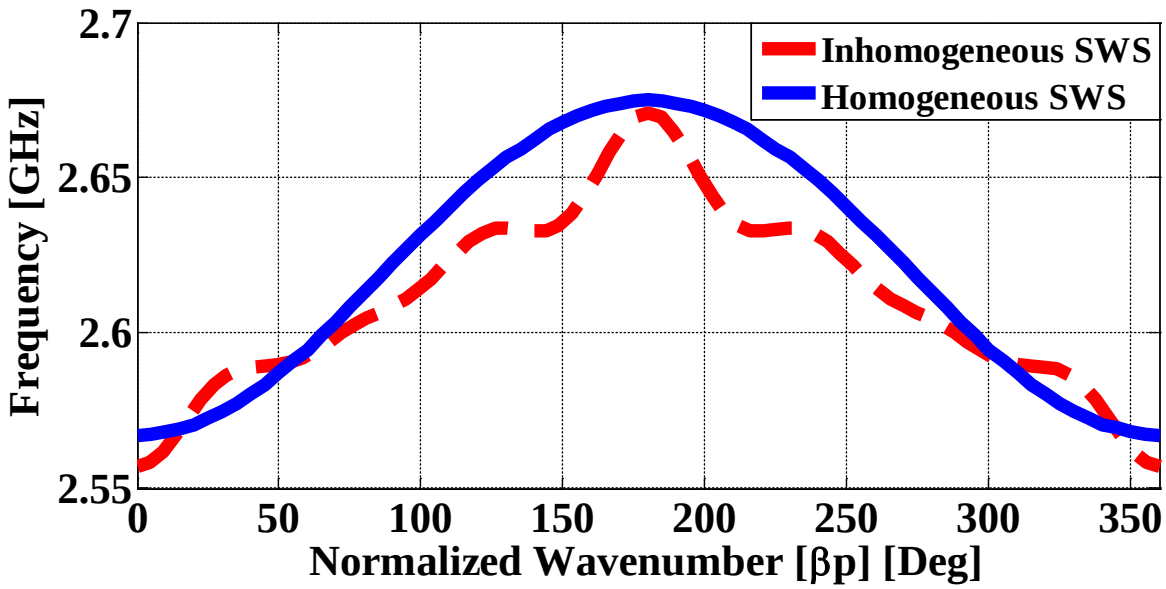

Fig.13: Measured dispersion curves of homogeneous and inhomogeneous SWSs. Inhomogeneous SWSs exhibit MSIPs

4.6 Hot Test Simulations

The impact of the efficiency enhancement techniques presented previously was investigated using the CST particle in cell (PIC) code. A high power electron beam guided by a static magnetic field was introduced into the SWS. The output power, output signal and its frequency spectrum were predicted using the PIC code. A Ka band design utilizing a 340 kV, 30A electron beam corresponding to an input beam power of 10.2 MW yielded 5.92 MW of output power at 27 GHz with 58% efficiency [34]. Utilizing the concepts of MSIPs and 3-section inhomogeneous SWSs, an S band design utilizing a 382 kV, 30A electron beam yielded 8.25 MW output power corresponding to 70% efficiency. Fig. 14 shows the output signal while Fig. 15 shows the output signal spectrum with high mode purity (single peak spectrum shows single mode operation). Fig. 16 shows the peak output power over time.

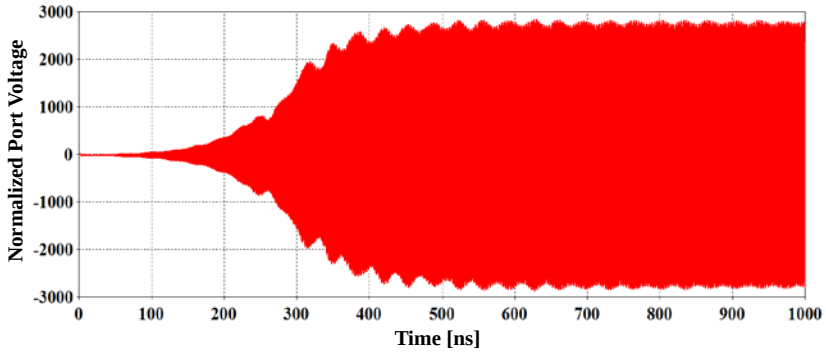

Fig.14: PIC simulation output port signal over time

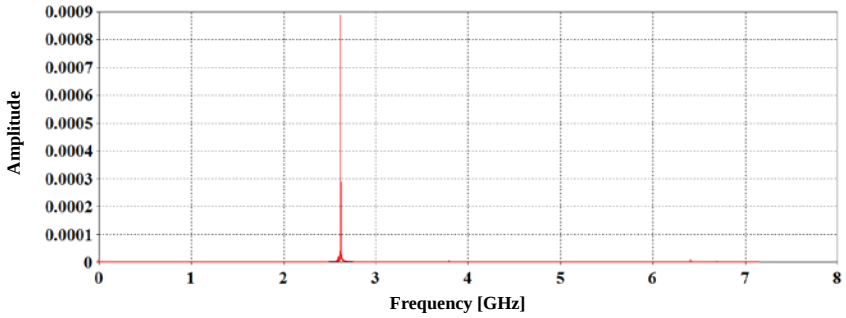

Fig.15: PIC simulation output port frequency spectrum

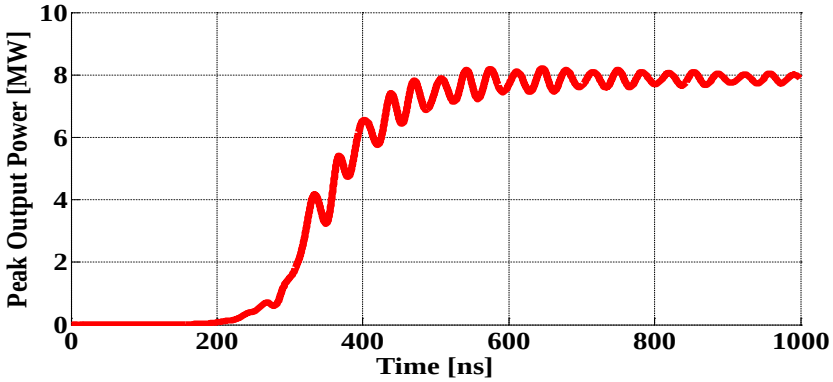

Fig.16: Peak output power over time.

5. References

[1] J. Zhang *et al*., "Recent advance in long-pulse hpm sources with repetitive operation in s-,c-, and x-bands," *IEEE Trans. Plasma Science*, vol. 39, pp. 1438-1445, June 2011.

[2] M. Yalandin, S. Rukin, V. Shpak, S. Shunailov, V. Rostov, and G. Mesyats, "Highly effective, repetitive nanosecond-range Ka-band bwo," *IEEE International Power Modulators and High Voltage Conference*, pp.402-404, May 2008.

[3] M Zhang *et al*., "A d-band backward wave oscillator based on quasi-parallel-plate slow wave structure," *Vacuum Electronics Conference (IVEC), 2015 IEEE International*, pp. 1-2 2015.

[4] Z. Wang *et al.*, "High –power millimeter-wave bwo driven by sheet electron beam," Electron Devices, IEEE Transactions on, vol. 60, no. 1, pp. 471-477, 2013.

[5] S.A. Kitsanov, A.I. Klimov, S.D. Korovin, I. K. Kurkan, I.V. Pegel and S.D. Polevin , " S-band resonant bwo with 5 gw pulse power," *High-Power Particle Beams (BEAMS), 2002 14th International Conference on*, vol. 1, pp. 255-258, June 2002.

[6] K. Dong, Y. Tang, and Y. Luo, "Design and simulation of a q-band gyrotron backward – wave oscillator with distributed loss," *IEEE Transactions on Plasma Science*, vol. 43, no. 8, pp. 2607-2612, 2015.

[7] C. Paolini et al., "THz backward-wave oscillators for plasma diagnostics in nuclear fusion," *IEEE Transactions on Plasma Science*, vol. 44, no. 4, pp. 369-376, 2016.

[8] M.R. Amin and K. Ogura, "Dispersion Characteristics of a rectangularly corrugated cylindrical slow wave structure driven by a non-relativistic annular electron beam," *IET Microwave Antennas Propagation*, vol. 1, no. 3, pp. 575-579, June 2007.

[9] J.J. Barroso, J.P. Leite and K.G. Kostov, "Cylindrical Waveguide with Axially Rippled Wall," *Journal of Microwaves and Optoelectronics*, vol. 2, no. 6, pp. 75-87, December 2002.

[10] J.P. Leite Neto and J.J. Barroso, "The sinusoidal as the longitudinal profile in backward wave oscillators of large cross sectional area," *Brazilian Journal of Physics*, vol. 34, no. 4B, pp. 1577-1581, December 2004.

[11] A.N. Vlasov et al., "Overmoded GW-Class surface wave microwave oscillator," *IEEE Trans. Plasma Science*, vol. 28, no. 3, pp. 550-560, June 2000.

[12] Z. Wang et al., "High-power millimeter-wave BWO driven by sheet electron beam," *IEEE Trans. Electron Devices*, vol. 60, no. 1, pp. 471-477, Jan. 2013.

[13] M.I. Yalandin et al., "Compact Ka-band backward-wave generator of superradiative pulses operating at reduced guiding magnetic field," *IEEE Trans. Plasma Sci*., vol. 36, no. 5, pp. 2604-2608, Oct. 2008.

[14] S.D. Korovin, S.D. Polevin, A.M. Roitman and V.V. Rostov, "Relativistic backward wave tube with nonuniform phase velocity of the synchronous harmonic," Russian Phys. J. vol.39, no. 12, pp. 1206-1209, 1996.

[15] L.D. Moreland et al., "Efficiency enhancement of high power vacuum BWOs using nonuniform slow wave structures," *IEEE Trans. Plasma Sci*., vol. 22, no. 5, pp. 554-565, Oct. 1994.

[16] J. H. Booske, “Plasma physics and related challenges of millimeter wave to terahertz and high power microwave generation,” *Physics of Plasmas* vol. 15, Feb 2008.
[17] R.J. Barker, J.H. Booske, N.C. Luhmann Jr, G.S. Nusinovich, *Modern Microwave and Millimeter wave Power Electronics*. Piscataway, NJ, USA: IEEE Press 2005.
[18] A.S. Gilmour Jr., *Klystrons, Travelling Wave Tubes, Magnetrons, Crossed-Field Amplifiers and Gyrotrons*. Norwood, Massachusetts, USA: Artech House 2011.

[19] L3 Electron Devices Product Catalogue: http://www2.l-3com.com/edd/products/r_klystrons.htm
[20] L3 Communications Product Catalogue: http://www2.l-3com.com/edd/products/r_magnetrons_s-band.htm
[21] L3 Communications Product Catalogue: http://www2.l-3com.com/edd/products/r_twt_hp.htm
[22] Communications and Power Industries (CPI) Product Catalogue: http://www.cpii.com/product.cfm/1/20/46
[23] Communications and Power Industries (CPI) Product Catalogue: http://www.cpii.com/product.cfm/1/17/118
[24] Communications and Power Industries (CPI) Product Catalogue: http://www.cpii.com/product.cfm/1/18/34
[25] G. S. Nusinovich, Y. Carmel, T. M. Antonsen, D. M. Goebel and J. Santoru, "Recent progress in the development of plasma-filled traveling-wave tubes and backward-wave oscillators," in *IEEE Transactions on Plasma Science*, vol. 26, no. 3, pp. 628-645, Jun 1998.
[26] X. Zhai, E. Garate, R. Prohaska, G. Benford and A. Fisher, "Experimental study of a plasma-filled backward wave oscillator," in *IEEE Transactions on Plasma Science*, vol. 21, no. 1, pp. 142-150, Feb 1993.
[27] C. Grabowski, J. M. Gahl and E. Schamiloglu, "Initial plasma-filled backward-wave oscillator experiments using a cathode-mounted plasma prefill source," in *IEEE Transactions on Plasma Science*, vol. 26, no. 3, pp. 653-668, Jun 1998.
[28] Y. Carmel, K. Minami, R. A. Kehs, W.W. Destler, V.L. Granatstein, D. Abe and W.L. Lou, “ Demonstration of efficiency enhancement in a high power backward wave oscillator by plasma injection,” *Phys. Rev Lett.*, vol. 62, pp. 2389-2392, 1989.
[29] B. Levush, T. M. Antonsen, A. Bromborsky, W. R. Lou and Y. Carmel, "Theory of relativistic backward-wave oscillators with end reflectors," in *IEEE Transactions on Plasma Science*, vol. 20, no. 3, pp. 263-280, Jun 1992.
[30] L. D. Moreland, E. Schamiloglu and R. W. Lemke, "Effects of end reflections on the performance of relativistic backward wave oscillators," *Pulsed Power Conference, 1995. Digest of Technical Papers., Tenth IEEE International*, Albuquerque, NM, USA, 1995, pp. 705-710 vol.1.
[31] D. M. Goebel, E. A. Adler, E. S. Ponti, J. R. Feicht, R. L. Eisenhart and R. W. Lemke, "Efficiency enhancement in high power backward-wave oscillators," in *IEEE Transactions on Plasma Science*, vol. 27, no. 3, pp. 800-809, Jun 1999.
[32] J. S. Hummelt, S. M. Lewis, M. A. Shapiro and R. J. Temkin, "Design of a Metamaterial-Based Backward-Wave Oscillator," in *IEEE Transactions on Plasma Science*, vol. 42, no. 4, pp. 930-936, April 2014.

[33] S. D. Korovin, S. D. Polevin, V. V. Rostov and A. M. Roitman, "The nonuniform-phase-velocity relativista BWO," *High-Power Particle Beams, 1992 9th International Conference on*, Washington,DC, 1992, pp. 1580-1585.
[34] U. Chipengo, M. Zuboraj, N. K. Nahar and J. L. Volakis, "A Novel Slow-Wave Structure for High-Power Ka -Band Backward Wave Oscillators With Mode Control," in *IEEE Transactions on Plasma Science*, vol. 43, no. 6, pp. 1879-1886, June 2015.
[35] J. W. Gewartowski and H.A. Watson, *Principles of Electron Tubes,* Princeton, New Jersey, USA, D. Van Nostrand Company, 1965.
[36] J.R. Pierce, Travelling Wave Tubes, Princeton, NJ, USA: Van Nostrand, 1950
[37] U. Chipengo, N. K. Nahar and J. L. Volakis, "Cold Test Validation of Novel Slow Wave Structure for High-Power Backward-Wave Oscillators," in *IEEE Transactions on Plasma Science*, vol. 44, no. 6, pp. 911-917, June 2016.
[38] H. Guo *et al*., "A novel highly accurate synthetic technique for determination of the dispersive characteristics in periodic slow wave circuits," in *IEEE Transactions on Microwave Theory and Techniques*, vol. 40, no. 11, pp. 2086-2094, Nov 1992.